Received: 20 March 2020 | Revised: 11 May 2020 | Accepted: 15 June 2020

DOI: 10.1002/bit.27468

ARTICLE

BIOTECHNOLOGY BIOENGINEERING WILEY

Bioprocess considerations for T-cell therapy: Investigating the impact of agitation, dissolved oxygen, and pH on T-cell expansion and differentiation

Arman Amini[1,2] | Vincent Wiegmann[1] | Hamza Patel[1] | Farlan Veraitch[1,2] | Frank Baganz[1]

[1]Department of Biochemical Engineering, The Advanced Centre for Biochemical Engineering, University College London, London, UK

[2]Oribiotech Ltd., London, UK

Correspondence
Frank Baganz, Department of Biochemical Engineering, The Advanced Centre for Biochemical Engineering, University College London, Torrington Place, London WC1E 7JE, UK.
Email: f.baganz@ucl.ac.uk

Funding information
UK Engineering and Physical Sciences Research Council (EPSRC), Grant/Award Numbers: EP/G034656/1, EP/P006485/1

Abstract

Adoptive T-cell therapy (ACT) has emerged as a promising new way to treat systemic cancers such as acute lymphoblastic leukemia. However, the robustness and reproducibility of the manufacturing process remains a challenge. Here, a single-use 24-well microbioreactor (micro-Matrix) was assessed for its use as a high-throughput screening tool to investigate the effect and the interaction of different shaking speeds, dissolved oxygen (DO), and pH levels on the growth and differentiation of primary T cells in a perfusion-mimic process. The full factorial design allowed for the generation of predictive models, which were used to find optimal culture conditions. Agitation was shown to play a fundamental role in the proliferation of T cells. A shaking speed of 200 rpm drastically improved the final viable cell concentration (VCC), while the viability was maintained above 90% throughout the cultivation. VCCs reached a maximum of 9.22×10^6 cells/ml. The distribution of CD8+ central memory T cells (T_{CM}), was found to be largely unaffected by the shaking speed. A clear interaction between pH and DO ($p < .001$) was established for the cell growth and the optimal culture conditions were identified for a combination of 200 rpm, 25% DO, and pH of 7.4. The combination of microbioreactor technology and Design of Experiment methodology provides a powerful tool to rapidly gain an understanding of the design space of the T-cell manufacturing process.

KEYWORDS

bioprocessing, immunotherapy, microbioreactor, perfusion mimic, T cell

1 | INTRODUCTION

Chimeric antigen receptor (CAR) T-cell therapy, a type of adoptive T-cell therapy, has emerged as a novel and successful therapy for treating systemic cancers such as acute lymphoblastic leukemia (ALL) and non-Hodgkin lymphoma (Kalos et al., 2011; Maude et al., 2014; Porter et al., 2015).

There are now over 800 recruiting clinical trials worldwide that test CAR T-cell therapy (clinicaltrials.gov, accessed 29 February 2020). These trials have stemmed from the promising results

Arman Amini and Vincent Wiegmann are considered joint first author.

generated from the two clinically approved CAR T-cell therapies, Kymeriah™ (Novartis), and Yescarta™ (Gilead/Kite).

Despite ongoing advances in T-cell and protein engineering in the immuno-oncology field, ex vivo manufacturing of T cells on a commercial scale with high reproducibility and robustness remains a challenge. Contributing factors include (a) patient-to-patient variability in starting materials, (b) labor-intensive processes and lack of automation, (c) limited process control and monitoring, (d) absence of standardization in manufacturing and quality control, and (e) limited understanding of critical process parameters and their impact on T-cell quality and growth.

Currently, clinical-grade primary T cells are manufactured in different platforms, including the CliniMACS prodigy system (Miltenyi Biotec Inc.), WAVE bioreactors (GE Healthcare Life Sciences), VueLife® Bags (CellGenix), and G-Rex cell culture flasks (Wilson Wolf; Iyer, Bowles, Kim, & Dulgar-Tulloch, 2018). Although these platforms are widely used, the impact of different process parameters including pH, dissolved oxygen (DO), and agitation on expansion and differentiation of T cells are yet to be fully characterized and understood.

Current protocols for the expansion of T cells often lack the active control of culture conditions such as DO and pH. Furthermore, ex vivo manufacturing conditions are typically different to T-cell activation and expansion conditions found in the human body. In vivo T cells are exposed to a wide range of pH and oxygen levels, with oxygen concentrations ranging from 0.2% to 3% in the thymus, 0.5–4.5% in spleen and lymph nodes to 13% in arterial blood (Caldwell et al., 2001; Carreau, Hafny-Rahbi, Matejuk, Grillon, & Kieda, 2011; Hale, Braun, Gwinn, Greer, & Dewhirst, 2002; McNamee, Korns Johnson, Homann, & Clambey, 2013). pH levels can vary from 7.4 in normal tissues to 6.7–6.9 in the tumor microenvironment (Corbet & Feron, 2017; Gerweck & Seetharaman, 1996).

Due to their ability to monitor and control relevant culture parameters at the small scale, microbioreactors have become an integral part of the bioprocess development timeline. Their utility has been demonstrated in a range of cell culture applications (Amanullah et al., 2010; Betts et al., 2014; Rameez, Mostafa, Miller, & Shukla, 2014). To unlock the full potential of the large amounts of data generated by these high-throughput systems, statistical tools such as design of experiment (DoE) are often used in conjunction (Hemmerich, Noack, Wiechert, & Oldiges, 2018; Sandner, Pybus, McCreath, & Glassey, 2019). However, few studies have utilized microbioreactors for the advancement of T-cell processes (Klarer, Smith, Cassidy, Heathman, & Rafiq, 2018) and to our knowledge, none have employed DoE approaches.

This study seeks to explore the impact of pH, DO, and agitation rate on the growth kinetics and phenotypic composition of primary T cells cultivated in the micro-Matrix microbioreactor with the aim to optimize these. By assessing the outlined design space with cells from three donors, the results hold a degree of universal validity and provide a more general insight into the response of T cells to their environmental conditions.

2 | MATERIALS AND METHODS

2.1 | Primary T-cell culture

Fresh and healthy donor blood was purchased from Cambridge Bioscience (Cambridge Bioscience, UK). Blood samples were collected under a comprehensive informed consent that permits the use of blood for research applications. Research Ethics Committee (REC) favorable opinion was obtained (REC reference: 17/SW/0189) before commencing the study. Peripheral blood mononuclear cells (PBMCs) were isolated from healthy donors' blood by Lymphoprep™ density gradient medium (Stemcell Technologies, Vancouver, Canada or Oslo, Norway). CD3+ cells were then isolated through negative selection using a Pan T Cell Negative Isolation Kit (Miltenyi Biotec, Bergisch Gladbach, Germany), according to the manufacturer's instruction. Primary PBMCs and T cells were kept in culture using RPMI-1640 (Gibco, Paisley, UK) with 10% heat-inactivated fetal bovine serum (FBS; Gibco), 2 mM glutamine (Gibco) and 1 mM sodium pyruvate (Gibco, Grand Island, NY). Pan T cells were seeded at 4×10^5 cells/ml in 2 ml of complete medium supplemented with 25 ng/ml of Interleukin 7 (IL-7; Miltenyi Biotec) and 10 ng/ml of interleukin-15 (Miltenyi Biotec). For activation of T cells, anti-CD3/CD28 expansion Dynabeads (Life Technologies AS, Norway) were washed and added to the cells in a Dynabead to cell ratio of 3:1.

2.2 | DoE methodology

A DoE approach was used to ascertain the effect of pH, DO, and shaking speed on T-cell expansion and differentiation. Using Design Expert v10 DoE software (Stat-Ease, Inc., MN), a factorial design was generated whereby each factor was varied over two levels (high and low) (Table 1). Each condition was repeated three times for each donor giving a total of nine replicates per condition (three donors used). Five center point replicates were also added per donor to check for curvature in the responses. The experimental runs were performed on the micro-Matrix platform. Table 2 summarizes the experimental design space.

To analyse the data, viable cell concentration and percentage of CD8+ T_{CM} cells from each run were entered into the Design Expert software. Data for each response factor was transformed as appropriate to approximate normal distribution (Guy, McCloskey, Lye, Mitrophanous, & Mukhopadhyay, 2013). The automatic model selection tool was used to keep only significant terms in the model. The criterion used was backward *p* value

TABLE 1 Table of factors evaluated for T-cell expansion

Factor	Name	Units	Low level (−)	High level (+)
A	pH	pH unit	6.9	7.4
B	DO	%	25	90
C	Shaking speed	rpm	100	200

TABLE 2 Experimental design space of two-level factorial design with five center points generated using Design Expert

Pattern	A: pH	B: DO	C: Shaking speed
−−−	6.9	25	100
+−−	7.4	25	100
−+−	6.9	90	100
−−+	6.9	25	200
++−	7.4	90	100
+−+	7.4	25	200
−++	6.9	90	200
+++	7.4	90	200
000	7.15	57.5	150

Note: Each condition was repeated three times for three separate donors.
Abbreviation: DO, dissolved oxygen.

selection set at a cut-off value of .1. Keeping only significant terms maximizes the resulting regression function of the model (Guy et al., 2013). The reduced model was analysed using analysis of variance (ANOVA) to ensure all the statistical parameters were within the appropriate limits. From the ANOVA, the lack of fit statistic was not significant and *F*-values for both models were large enough to indicate adequate signal and reject the effect of noise. All the other outputs from the ANOVA suggested the models for both responses were significant.

2.3 | micro-Matrix set-up and operation

The micro-Matrix microbioreactor (Applikon-Biotechnology, the Netherlands) was used for all T-cell cultivations. A detailed account of how the micro-Matrix can be set up and operated for cell cultivations is given in Wiegmann, Martinez, and Baganz (2020). Briefly, before each run, the pH sensors in the micro-Matrix cassette were recalibrated by first filling each well with 2 ml of 0.2 µm sterile filtered 1× phosphate-buffered saline (PBS; Life Technologies, Paisley, UK) and then mounting the cassette onto the micro-Matrix system to initiate pH readings via the control software. Readings were taken at room temperature, with neither shaking motion nor gas supply for at least 60 min. After stabilization of the pH measurements, 1 ml was aseptically extracted from three representative wells and then analysed using an offline pH meter (Mettler Toledo, Leicester, UK). The average pH of these readings was used to define the offset for each well. Following the removal of 1× PBS, each well was inoculated with 2 ml of the previously prepared cell suspension at a concentration of 5×10^5 cells/ml, before starting the cultivation. The maximum gas flow rate was set to 1.4 ml/min, the shaking speed was set to either 100 or 200 rpm, and the temperature was controlled at 37°C. Control of the pH was achieved through overlay with CO_2 and scheduled manual bolus additions of sodium bicarbonate buffer (250 mM $NaHCO_3$ and 250 mM Na_2CO_3). The control of the DO was achieved through overlay with O_2 and N_2. Bolus additions of 100 µl of sterile filtered deionised (DI) water were made every second day to counteract evaporation. After 4 days of cultivation, the volume in each well was measured using serological pipettes and topped up to 2 ml with 0.2 µm sterile filtered DI water if necessary.

2.4 | Perfusion mimic

To perform the medium exchange while retaining the cells in culture, the cassette was removed from the micro-Matrix and transferred to a Centrifuge 5810 R (Eppendorf, Hamburg, Germany). After pelleting the cells for 3 min at 200 *g*, half of the supernatant was removed aseptically and replaced with the supplemented medium. Aliquots of the cytokines were thawed on the day of their use (storage at −18°C). For the higher perfusion rate of 1.0 vessel volume per day (VVD), this procedure was performed twice daily with the period between medium exchanges being no shorter than 7 hr and no longer than 16 hr.

2.5 | Cell count and metabolite analyses

Following Day 3, 100 µl of cell suspension were extracted daily and analysed for cell concentration and viability using Via1-Cassettes in combination with a NucleoCounter NC-3000 (both ChemoMetec, Allerod, Denmark). The supernatant that was extracted as part of the medium exchange was analysed for nutrients and metabolites using a Bioprofile FLEX (Nova Biomedical, Waltham, MA). The viable cell number and metabolite data were then used to calculate the specific metabolite consumption rates as described by Sewell et al. (2019). Equation (1) was used to calculate specific rates during the perfusion mimic cultivations:

$$q_{\text{Met}} = \frac{(c_{i-1} \cdot (1 - D) + (c_{\text{Medium}} \cdot D)) - c_i}{\Delta \text{IVCC}_i}. \quad (1)$$

where c_i is the concentration of the nutrient or metabolite in the cultivation broth at t_i, c_{i-1} is the concentration of the nutrient or metabolite in the cultivation broth at t_{i-1}, c_{Medium} is the concentration of the nutrient or metabolite in the medium, and D is the dilution rate. The IVCC was calculated according to Equation (2):

$$\text{IVCC} = \frac{x_i + x_{i-1}}{2} \cdot \left(t_i - t_{i-1}\right). \quad (2)$$

where x_i is the viable cell concentration (VCC) at t_i and x_{i-1} is the VCC at t_{i-1}. The lactate yield was calculated using Equation (3):

$$Y_{\text{Lac/Gluc}} = \frac{q_{\text{Lac}}}{q_{\text{Gluc}}}, \quad (3)$$

where q_{Lac} and q_{Gluc} are the specific rates of lactate production and glucose consumption, respectively.

2.6 | Flow cytometry

For phenotypic characterization of T cells on Day 8, cells were labeled with the following primary antibodies (Becton Dickinson): CD3-BUV305, CD4-BUV805, CD8-BUV737, CCR7-BV421, and CD45RO-PE-Cy7. Fluorescence was measured on a 5-laser LSRFortessa-X20 flow cytometer (BD Biosciences) and analysed using FlowJo v10 (FlowJo LLC, OR).

2.7 | Statistical analysis

All statistical analyses were performed using Prism 7 (GraphPad, San Diego, CA). The minimal level of confidence at which the results were considered significant was $p < .05$. Statistical significance was determined by two-way ANOVA with post hoc Tukey's multiple comparison test.

3 | RESULTS

After isolation of T cells from fresh PBMC from three different healthy donors, T cells were seeded at 4.0×10^5 cells/ml activated by Dynabeads (Figure 1a). The factors agitation, pH, and DO were investigated as they form the basis of a controlled bioprocess. Two agitation speeds were tested to explore a low-shear, but poorly mixed environment at 100 rpm and a well-mixed, but higher shear environment at 200 rpm. A DO setpoint of 25% air saturation was selected to recreate physiological oxygen tension in lymphoid tissues (Caldwell et al., 2001), whereas a DO of 90% air saturation more resembles the level of oxygen that cells are exposed to during in vitro cell culture in 5% CO_2 incubators (Wenger, Kurtcuoglu, Scholz, Marti, & Hoogewijs, 2015). Similarly, a neutral pH of 7.4 was tested as it resembles the pH environment in healthy tissues (Erra Díaz, Dantas, & Geffner, 2018; Gerweck & Seetharaman, 1996; Mordon, Maunoury, Devoisselle, Abbas, & Coustaud, 1992), whereas a pH of 6.9 is more representative of a cultivation under uncontrolled incubator conditions in which the medium acidifies as a result of lactic acid production (Costariol et al., 2019).

3.1 | Growth kinetics

As illustrated in Figure 1b, the cells were subject to an extended lag period in the initial 72 hr of the cultivation. Subsequently, cell growth accelerated to a varying degree depending on the condition tested. A higher shaking speed of 200 rpm improved cell growth and the cells were still in the exponential growth phase at the end of the experiment. With this in mind, a higher shaking speed may predict an even further increase in cell densities within extended cultivation times. The highest cell density achieved was 9.22×10^6 cells/ml (200 rpm, DO 25%, and pH 6.9). In most cases, a shaking speed of 100 rpm restrained growth and cells entered the stationary phase towards the end of the run. The lowest final cell density obtained was 1.26×10^6 cells/ml (100 rpm, DO 90%, and pH 6.9). A similar trend is demonstrated by the final fold expansion (Figure 1c).

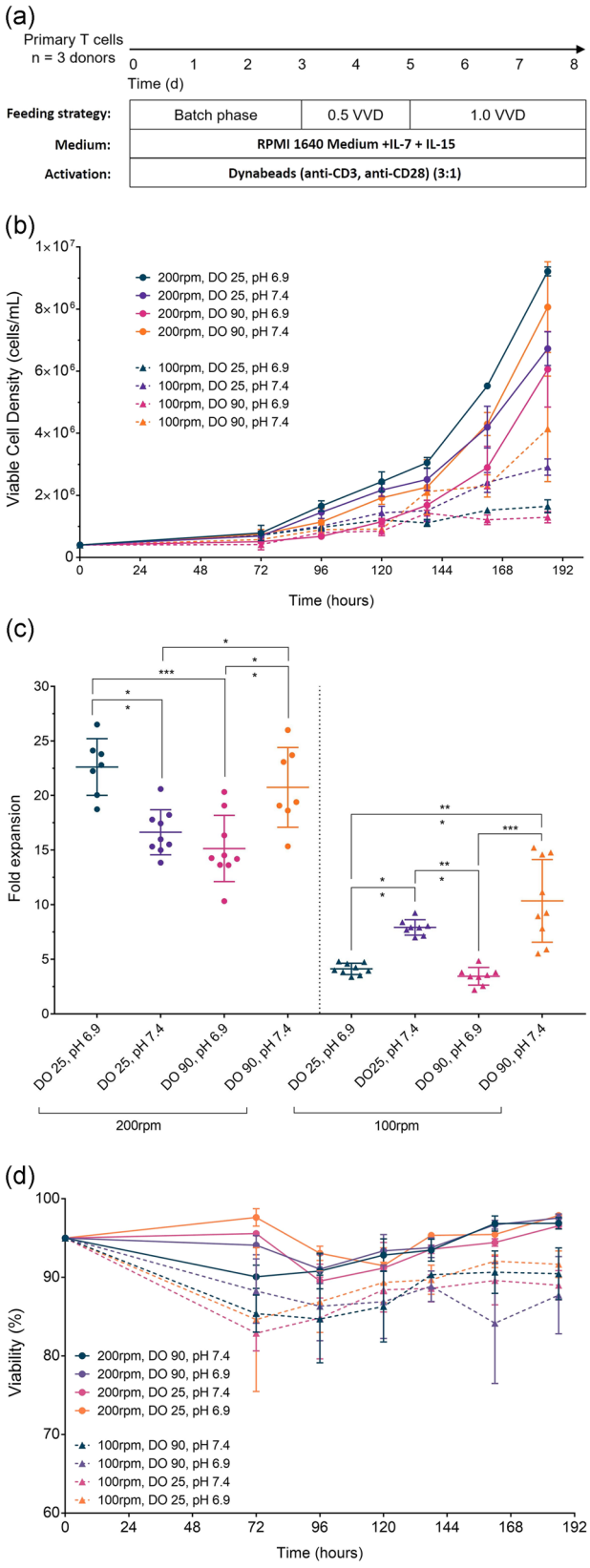

A similar discrepancy between higher and lower shaking speeds could be observed for the viability (Figure 1d). Whereas a viability of greater than 90% was maintained throughout the culture for the conditions of high shaking speeds, at 100 rpm the viability dropped to 80–90% on Day 3 and then steadily recovered to roughly 90% on Day 8.

Additionally, it was found that the cells were not homogeneously suspended at 100 rpm. Instead, large cell aggregates formed in the center of the well, whereas a homogenous cell suspension was found at 200 rpm (data not shown).

3.2 | Metabolites

Figure 2 shows the specific glucose consumption and lactate production rates for all conditions tested. The condition with the highest fold expansion (200 rpm, DO 25%, and pH 6.9) also showed the lowest specific glucose consumption, whereas the condition with the lowest fold expansion (100 rpm, DO 90%, and pH 6.9) showed the highest specific glucose consumption (Figure 2a). These results may imply that fast-growing T cells may inhabit a different metabolic state when compared with slow-growing cells.

Generally, this trend was reversed for the specific lactate production. A higher shaking speed of 200 rpm promoted a higher production rate of lactate per cell compared to 100 rpm. Additionally, the pH played an important role in the generation of lactate at a shaking speed of 100 rpm. A low pH setpoint significantly reduced the production of lactate compared with the higher pH setpoint. At a shaking speed of 200 rpm, however, the DO setpoint was found to have a greater effect on the lactate production, and a higher DO generally led to increased lactate production rates (Figure 2b).

To further investigate the glycolysis activity of the cells, the lactate yield was calculated. In a purely glycolytic environment, the theoretical lactate yield equals a value of 2. This means that two moles of lactate are generated for each mole of glucose. All tested conditions fall well below this value (Figure 2c). At 100 rpm, a clear correlation to the pH can be observed that determines how the cells utilize glucose. At 200 rpm, however, no such correlation exists for the pH and the DO setpoint appears to have a more pronounced effect. The progression of glucose and lactate concentrations over the course of the cultivation can be found in the Figure S1.

FIGURE 1 Process flowsheet of the cultivation of primary T cells grown in the micro-Matrix using a perfusion-mimic methodology (a). Growth (b), fold expansion (c), and viability (d) throughout the cultivation of primary T cells under varying parameter combinations for shaking speed, pH, and DO, a temperature of 37°C, and a working volume of 2 ml. Mean ± *SD* of three healthy donors with two to six replicates each. Significance is indicated when $*p \leq .05$, $**p \leq .01$, $***p \leq .001$. DO, dissolved oxygen; *SD*, standard deviation [Color figure can be viewed at wileyonlinelibrary.com]

3.3 | Immunophenotypic analysis

The cell population was analysed to characterize the CD4:CD8 ratio and subpopulations of CD8 cells before and after 8 days of cultivation (Figures S2 and 3). The less differentiated T_{CM} (CCR7+CD45RO

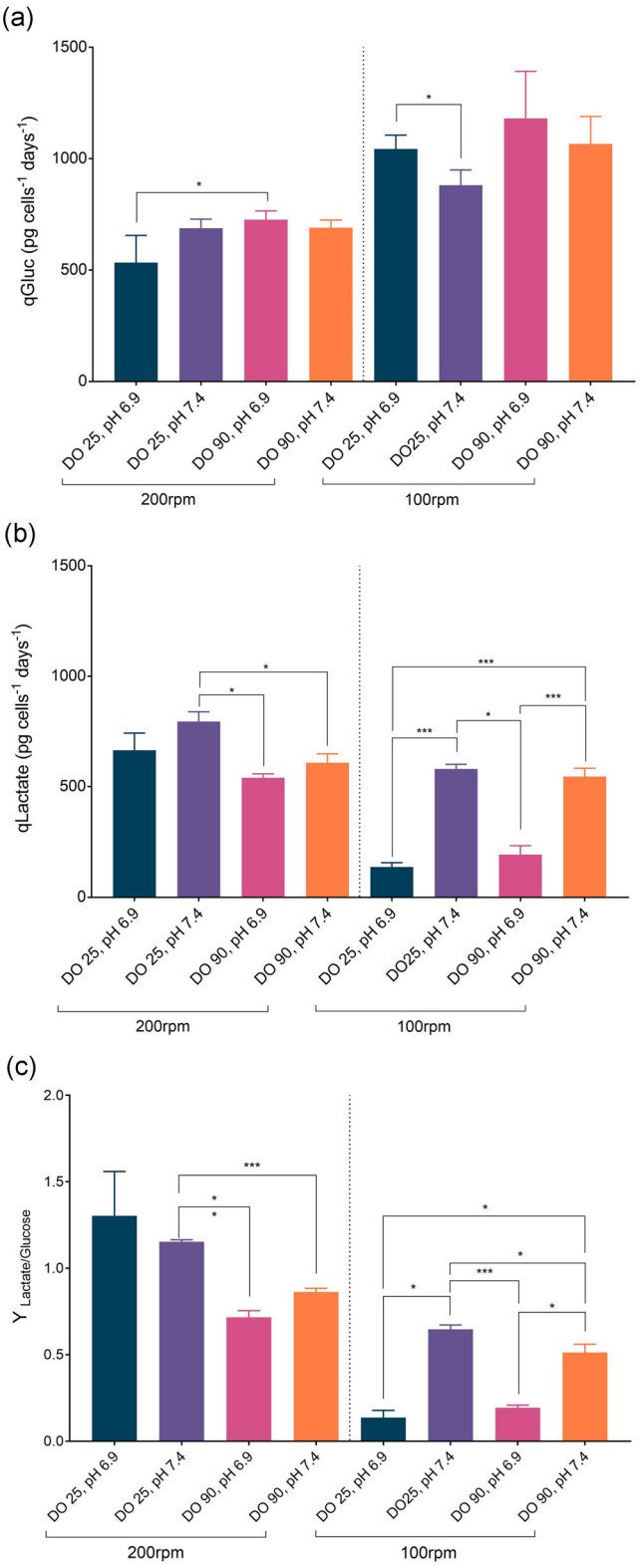

+) are considered clinically preferable compared with the more differentiated effector memory T cells (T_{EM}; CCR7+CD45RO+), mainly due to the greater in vivo proliferative capacity, longevity and persistence of T_{CM} cells (Kochenderfer et al., 2017; Louis et al., 2011; Sallusto, Lenig, Förster, Lipp, & Lanzavecchia, 1999). The highest percentage of T_{CM} cells (Figure 3a) of 32.6 ± 11.3% was achieved at DO 25% and pH 7.4. This combination of DO and pH also favored T_{CM} cells at 100 rpm with a percentage of 24.4 ± 5.8%. At 200 rpm, the lowest concentrations of T_{CM} cells corresponded to the conditions that had the highest fold expansion (DO 25%, pH 6.9 and DO 90%, pH 7.4). These combinations of DO and pH also lead to the lowest percentages of T_{CM} cells at 100 rpm. As anticipated, this pattern is largely inverted when examining the percentage of T_{EM} cells (Figure 3b).

The ratio of CD4:CD8 (Figure 3c) was subject to high donor-to-donor variability, as one of the three donors showed a consistently reduced percentage of CD8 cells. Although no significant differences could be observed between the tested conditions, the low DO set-point at 100 rpm might show a tendency to increase the CD4:CD8 ratio.

3.4 | DoE model evaluation

The two response factors analysed using Design Expert were final VCC and percentage of CD8+ T_{CM} cells. The respective model graphs are illustrated in Figure 4a,b. In terms of VCC, the software identified only two significant factors for this model, shaking speed and pH. DO was found to have no significant effect and was thus removed from the model by backward *p* value elimination. Between the two factors, shaking speed had a stronger effect on the VCC model compared to pH. As shown in Figure 4a, the progression of color on the contour map changes significantly from blue (low VCC) to red (high VCC) as the shaking speed increased from 100 to 200 rpm. Furthermore, VCC is independent of pH at high shaking speeds, that is, the red area corresponding to high VCC is apparent at both high and low pH. The effect of pH is observed at low shaking speeds. Here, a higher pH is desired as seen by the color progression from blue (low VCC) to green (moderate VCC) as pH is increased from 6.9 to 7.4.

In terms of percentage of CD8+ T_{CM} cells, the software identified only two significant terms to have a strong effect on the model, DO and pH. Shaking speed was a nonsignificant term and was thus removed from the model by backward *p* value elimination as before. According to Figure 4b, it seems that both pH and DO have an equally strong effect on the percentage of CD8+ T_{CM} cells. Conditions of low DO and high pH achieve the highest concentration of

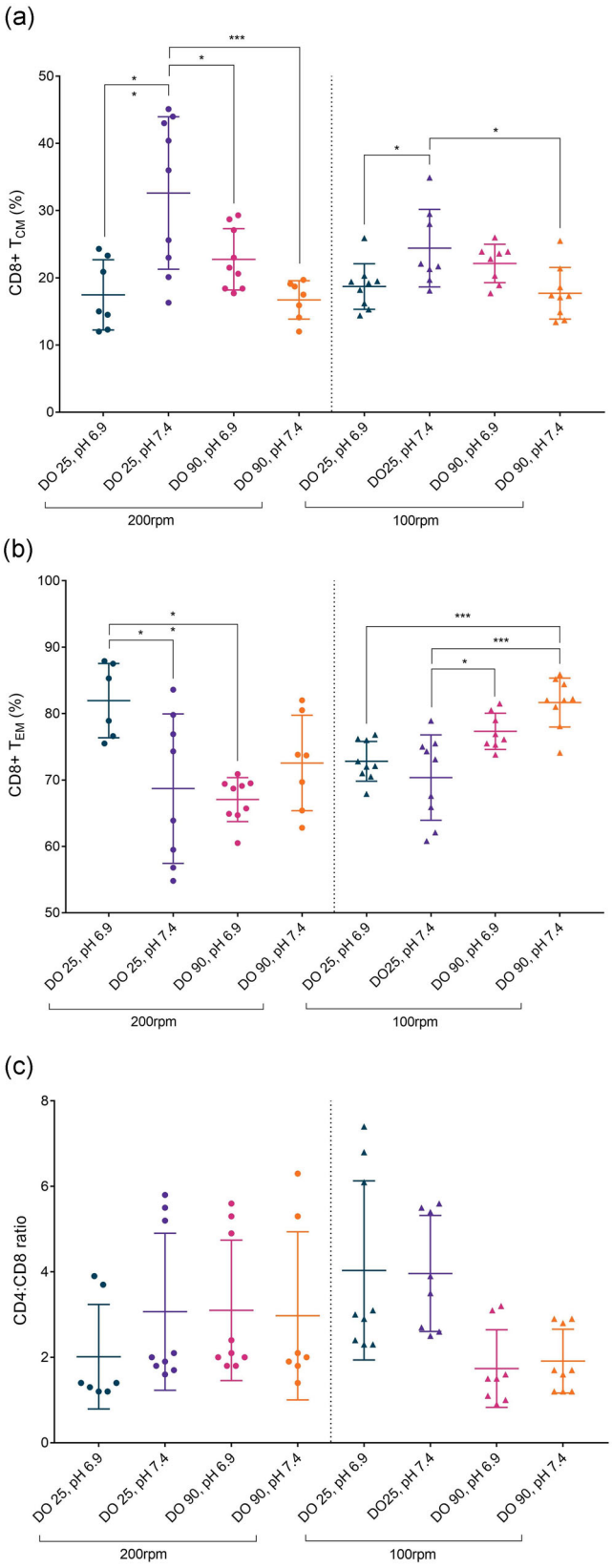

FIGURE 2 Cell specific glucose consumption rates (a), lactate production rates (b), and lactate yield (c) of primary T cells grown in the micro-Matrix at different combinations of shaking speed, pH, and DO using perfusion mimic as mode of operation. For all conditions, the temperature was controlled at 37°C and the working volume was 2 ml. Mean ± *SD* of three healthy donors with two to six replicates each. Statistical comparisons were done using Tukey's multiple comparison test. Significance is indicated when $^{*}p \leq .05$, $^{**}p \leq .01$, $^{***}p \leq .001$. DO, dissolved oxygen; *SD*, standard deviation [Color figure can be viewed at wileyonlinelibrary.com]

CD8+ T_{CM} cells. On the contrary, a combination of high pH/high DO and low pH/low DO achieve comparably lower concentration of CD8+ T_{CM} cells.

On the basis of the DoE models, the numerical optimization tool in Design Expert was used to determine the operating condition that results in a high final cell density, but also a favorable phenotypic distribution. The numerical optimization tool combines the desired goal of those response factors into an overall desirability function, which the program then seeks to maximize. Desirability ranges from zero outside of the limits to one at the goal. The output from the optimization is illustrated graphically in Figure 5.

4 | DISCUSSION

4.1 | Agitation

The results demonstrate a distinctly positive effect of agitation on the proliferation of primary T cells grown in the micro-Matrix. An increased shaking speed is generally linked to better mixing and improved oxygen transfer, both of which are important for the cultivation of mammalian cells (Barrett, Wu, Zhang, Levy, & Lye, 2010; Betts et al., 2014; Wutz, Steiner, Assfalg, & Wucherpfennig, 2018). An additional factor for the expansion of T cells is their activation through Dynabeads present in the medium. Dynabeads are microscopic spheres coated with anti-CD3 and anti-CD28 antibodies. Cellular interaction with these antibodies is a strong stimulus that encourages T cells to proliferate in vitro (Kershaw, Westwood, & Darcy, 2013). To successfully activate T cells, Dynabeads must first collide and bind with the cells. This is a stochastic event driven by the fluid dynamics of the growth medium and has been demonstrated in a study by Costariol et al. (2019), where better growth was attributed to increased bead–cell interactions caused by higher stirrer speeds. Compared to the ambr 250 system used by Costariol et al. (2019), the working volume of the micro-Matrix is considerably lower and the mode of agitation is shaken instead of stirred. Nevertheless, a similar explanation may be applicable to the findings of this study.

In addition, large cell aggregates formed at the bottom of the well at a shaking speed of 100 rpm. Dependent on the size of the

FIGURE 3 CD8+ T central memory cells (a), CD8+ T effector memory cells (b), and CD4 to CD8 ratio (c) after 8 days of expansion in the micro-Matrix at different combinations of shaking speed, pH, and DO, using perfusion mimic as mode of operation. For all conditions, the temperature was controlled at 37°C and the working volume was 2 ml. Mean ± *SD* of three healthy donors with two to six replicates each. Statistical comparisons were done using Tukey's multiple comparison test. Significance is indicated when $^{*}p \leq .05$, $^{**}p \leq .01$, $^{***}p \leq .001$. DO, dissolved oxygen; *SD*, standard deviation [Color figure can be viewed at wileyonlinelibrary.com]

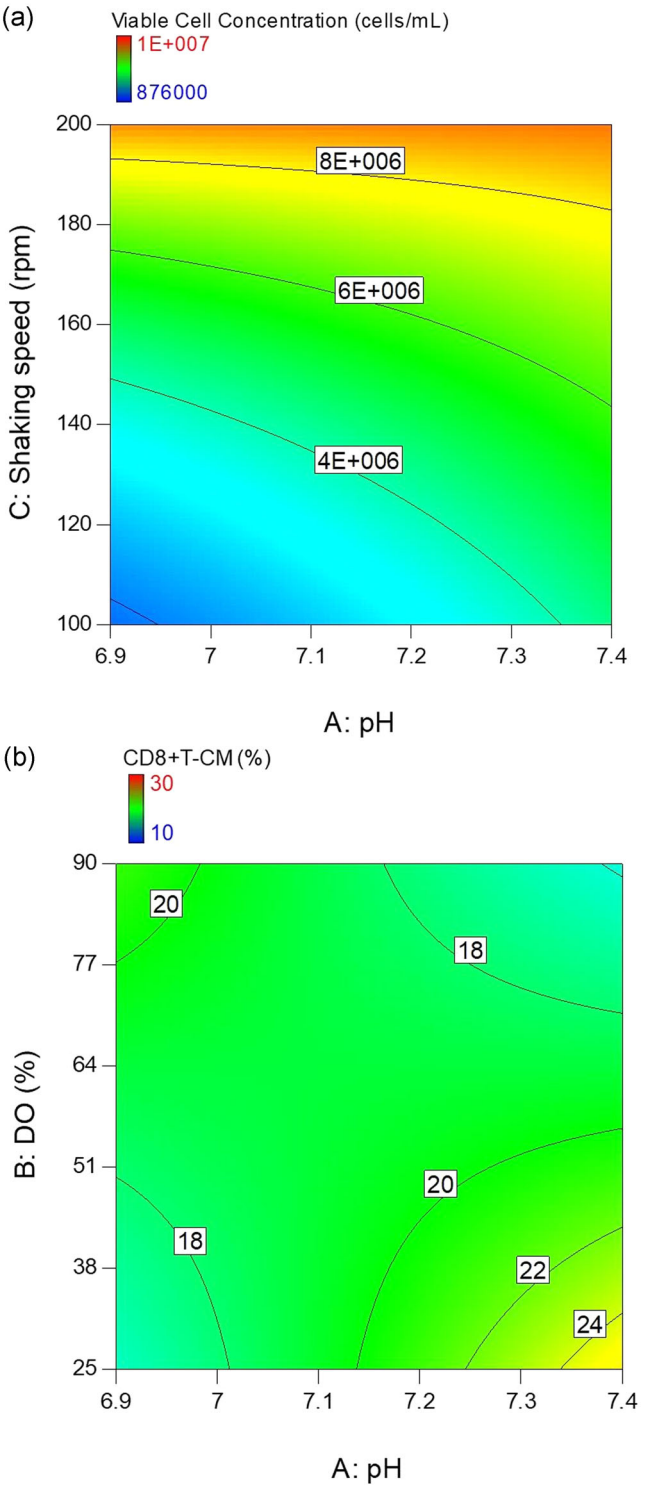

FIGURE 4 DoE models for viable cell concentration and percentage of CD8+ T_{CM} generated using Design Expert. Contour plot showing effect of pH and shaking speed on viable cell concentration (a). Contour plot showing effect of pH and DO on percentage of CD8+ T_{CM} cells (b). DO, dissolved oxygen; DoE, design of experiment [Color figure can be viewed at wileyonlinelibrary.com]

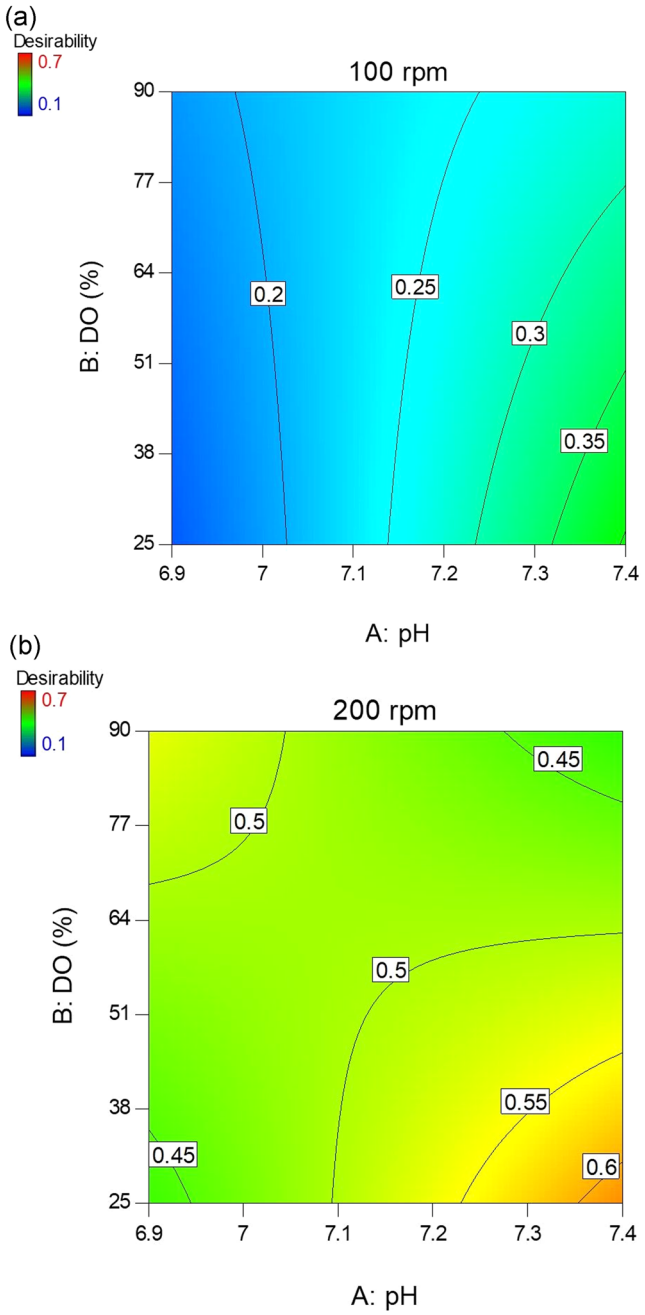

FIGURE 5 Numerical optimization of process conditions to maximize total cell numbers and phenotypic distribution. Contour map shows the desirability against pH and DO at fixed shaking speeds. 100 rpm (a) and 200 rpm (b). DO, dissolved oxygen [Color figure can be viewed at wileyonlinelibrary.com]

aggregates, cells that are part of these structures may be subject to severe transport limitations and by extension, variations in pH, DO, nutrients, and waste metabolites. This potentially explains the high glucose consumption rate at 100 rpm, since a stabilization of the hypoxia-inducible factor 1α due to hypoxia, increases glucose uptake and results in a metabolic shift from oxidative phosphorylation to glycolysis (Finlay et al., 2012; Kim, Tchernyshyov, Semenza, & Dang, 2006). Furthermore, bead–cell interactions may also be insufficient inside such aggregates.

In light of emerging off-the-shelf allogeneic T-cell therapies (Gouble et al., 2014), process scalability becomes an important consideration. It is therefore critical to investigate how the findings regarding aggregate formation and lack of Dynabead suspension translate to larger scale cultivation systems. Furthermore, a translation of the perfusion-mimic procedure may not be feasible at the large scale. At scale, additional cell separation equipment based on either spinning membrane filtration, alternating tangential flow, or acoustic separation could be employed in conjunction with the bioreactors, as scalability of the perfusion-mimic procedure has been demonstrated previously (Kelly et al., 2018; Klarer, Marsh, Ranade, & Smith, 2017; Kreye et al., 2019; Sewell et al., 2019).

4.2 | Effect of DO

The concentration of DO is an important process parameter routinely monitored and controlled in biopharmaceutical production processes. Its effect on the expansion of primary T cells in the micro-Matrix, however, was critically dependent on the other process parameters tested. A change of DO had no effect on cell growth at 100 rpm, whereas the effect was highly pH dependent at 200 rpm. Growth was improved at high DO and high pH (DO 90% and pH 7.4) as well as low DO and low pH (DO 25% and pH 6.9).

The current literature available presents a similarly ambiguous picture concerning the cultivation of T cells at varying pH levels. Human T cells grown in spinner flasks with a controlled pH of 7.2 demonstrated better growth at DO levels ranging from 5% to 50%, compared with 75% (Bohnenkamp, Hilbert, & Noll, 2002). In another study, atmospheric oxygen levels have been found to improve fold expansion by 50% compared with physiological oxygen levels (Atkuri, Herzenberg, & Herzenberg, 2005; Atkuri, Herzenberg, Niemi, Cowan, & Herzenberg, 2007). This was most likely due to an increase in intracellular nitric oxide and reactive oxygen species at the physiological oxygen level (McLaughlin & Demple, 2005). Another study found the same effect, but attributed the slow growth at physiological DO to a build-up of cAMP, which in turn, resulted in reduced T-cell activation due to lymphocyte-specific protein tyrosine kinase (Lck) inhibition (Larbi, Zelba, Goldeck, & Pawelec, 2010). In contrast, a study by Berahovich et al. (2019) found no differences in the expansion of T cells and CD19 CAR-T cells when cultured at physiological and atmospheric oxygen conditions.

The phenotypical distribution in this study was shown to be highest in CD8 T_{CM} cells when the DO was controlled at 25% and the pH was set to 7.4. Thus far, most studies show no effect of the DO on the differentiation of T cells and CD19 CAR-T cells (Atkuri et al., 2007; Berahovich et al., 2019). However, it is important to note that the majority of the referenced studies were not done under pH controlled or agitated conditions.

pH	DO (%)	Shaking speed (rpm)	Viable cell density (cells/ml)	CD8+ T_{CM} (%)	Desirability
7.4	25	200	9.01E06	25.5	0.620

TABLE 3 Highest ranking set of conditions from numerical optimization to maximize total cell numbers and phenotypic distribution

4.3 | Effect of pH

In this study, the growth of primary T cells was shown to be improved at a high pH of 7.4 when the shaking speed was set to 100 rpm. At 200 rpm, an interaction effect between pH and DO was found and a high pH was only favorable when coupled with a high DO of 90%. Literature that investigates the effect of pH on the expansion of T cells is limited and, in addition, these studies are usually conducted under semi-controlled incubator conditions without agitation. A study performed in T-flasks compared the fold expansion between T cells grown at pH levels between 7.0 and 7.4 and found that proliferation was best below pH 7.4 (Carswell & Papoutsakis, 2000). Furthermore, Bohnenkamp et al. (2002) showed that growth of T cells in a stirred bioreactor was slower in acidic condition (pH 6.7) and suggested the optimal range for T-cell expansion is between pH 7 and 7.3. Similarly, Calcinotto et al. (2012) expanded T cells in a broader range of pH levels between 6.5 and 7.4 and found that growth is impaired at the acidic end of the spectrum.

Furthermore, a low pH value of 6.9 appears to affect the metabolism by lowering the specific lactate production. This finding is supported by Pilon-Thomas et al. (2016), where acidic conditions led to a decrease in the glycolytic activity of T cells. A possible mechanism for the decreased lactate generation at elevated extracellular H^+ levels has been described for other cell types, where protons function as inhibitors of the enzyme phosphofructokinase, which plays a pivotal role in the glycolysis pathway (Dobson, Yamamoto, & Hochachka, 1986; Erecińska, Deas, & Silver, 2002; Halperin, Connors, Relman, & Karnovsky, 1969; Trivedi & Danforth, 1966).

A contributing factor could be the use of CO_2 overlay for the control of the pH. As the concentration of dissolved CO_2 has repeatedly been shown to distinctly affect growth and metabolism of other mammalian cell types, the potential impact of differing pCO_2 levels has to be acknowledged (Darja et al., 2016; Kimura & Miller, 1996; Xu et al., 2018; Zhu et al., 2008). The concentration difference of dissolved CO_2 would have been greatest at the beginning of the cultivation when a large amount of CO_2 was required to lower the pH to 6.9. In later stages of the cultivation, the accumulation of lactate sufficiently acidifies the medium, and no further CO_2 additions are necessary to control the pH. However, no measurements of the pCO_2 are available for these experiments due to the limited culture volume.

4.4 | Optimal culture conditions

Current manufacturing processes of adoptive T-cell therapies are still prohibitively expensive (Roddie, O'Reilly, Dias Alves Pinto, Vispute, & Lowdell, 2019). A more efficient and robust T-cell expansion step has the potential to drive down the overall cost of goods for such therapies. This study demonstrates that agitation is pivotal in reaching high cell densities. The final viable cell density not only determines the possible therapeutic dose, but an improved cell growth can also decrease the duration of the expansion and in turn, allow for an increased number of batches per year.

The success of the T-cell expansion, however, is not only measured by achieving a high number of cells, but also by the phenotypic distribution of the resulting cell population. Several studies suggest that in vivo efficacy, longevity, and proliferative capacity are highest for less differentiated phenotypes such as T_{CM} cells (Biasco et al., 2015; Gattinoni et al., 2011; Wang et al., 2016). The optimal set of conditions that achieved the highest desirability are shown in Table 3. The combination of these parameters achieved the best compromise in maximizing both viable cell concentration and percentage of CD8+ T_{CM} cells within the investigated design space. Furthermore, in this study all conditions were tested using RPMI-1640 medium supplemented with 10% FBS, which is widely used in immunological studies. High percentages of FBS (5–10%) are often used as RPMI-1640 lacks essential components for T-cell growth such as insulin, transferrin, and selenium. In the cancer immunotherapy field, often more complex media with 5% of human AB serum are being used (Medvec et al., 2018), since they provide a superior expansion while maintaining memory phenotype compared with RPMI-1640 (Pampusch et al., 2020).

Therefore, the identified optimal conditions in this study can be further improved by using more complex serum free media.

5 | CONCLUSION

This study investigated the effect of shaking speed, DO, and pH on the growth kinetics, metabolism, and the differentiation of primary T cells in vitro. Although significant effects of pH and DO on cell growth and differentiation could be established, they were less pronounced than in the case of agitation. Interestingly, a low pH value of 6.9 reduced the cell specific production of lactate. Processes with excessive build-up of lactate, therefore, may benefit from a low pH setpoint. Similarly, perfusion-mimic as mode of operation was effective at maintaining lactate concentrations below cytotoxic levels and glucose concentrations above depletion level.

The results highlight the potential that monitoring and control can bring to T-cell manufacturing and suggests a combination of process parameter setpoints that result in a high final cell density and high percentage of CD8 T_{CM} cells. The micro-Matrix proved to be a suitable tool for the rapid process development of T-cell manufacturing. The culture volume was small enough to allow for a high degree of parallelization, yet sufficient for a regular analysis of cell count and metabolic profile. The combination of high-throughput

screening tools such as the micro-Matrix and DoE methodology presents a promising approach for identifying and optimizing critical process parameters in cell and gene therapy manufacturing.

ACKNOWLEDGMENTS

This study was supported by the UK Engineering and Physical Sciences Research Council (EPSRC) Industrial Doctorate Training Centre (IDTC) in Bioprocess Engineering Leadership (EP/G034656/1). V. W. would also like to thank Applikon Biotechnology for additional financial support of his EngD studentship.

A. A. would also like to acknowledge the funding and support of the UK Engineering and Physical Sciences Research Council (EPSRC) through the Future Targeted Healthcare Manufacturing Hub hosted at University College London with UK university partners (Grant Reference: EP/P006485/1).

CONFLICT OF INTERESTS

The authors declare that there are no conflict of interests.

ORCID

Arman Amini https://orcid.org/0000-0001-9967-0749
Vincent Wiegmann https://orcid.org/0000-0001-6210-9296
Hamza Patel https://orcid.org/0000-0001-6105-5644
Farlan Veraitch https://orcid.org/0000-0001-8635-7024
Frank Baganz http://orcid.org/0000-0001-5589-6869

REFERENCES

Amanullah, A., Otero, J. M., Mikola, M., Hsu, A., Zhang, J., Aunins, J., … Russo, A. P. (2010). Novel micro-bioreactor high throughput technology for cell culture process development: Reproducibility and scalability assessment of fed-batch CHO cultures. *Biotechnology and Bioengineering*, *106*, 57–67.

Atkuri, K. R., Herzenberg, L. A., & Herzenberg, L. A. (2005). Culturing at atmospheric oxygen levels impacts lymphocyte function. *Proceedings of the National Academy of Sciences of the United States of America*, *102*, 3756–3759.

Atkuri, K. R., Herzenberg, L. A., Niemi, A.-K., Cowan, T., & Herzenberg, L. A. (2007). Importance of culturing primary lymphocytes at physiological oxygen levels. *Proceedings of the National Academy of Sciences of the United States of America*, *104*, 4547–4552.

Barrett, T. A., Wu, A., Zhang, H., Levy, M. S., & Lye, G. J. (2010). Microwell engineering characterization for mammalian cell culture process development. *Biotechnology and Bioengineering*, *105*, 260–275. https://doi.org/10.1002/bit.22531

Berahovich, R., Liu, X., Zhou, H., Tsadik, E., Xu, S., Golubovskaya, V., & Wu, L. (2019). Hypoxia selectively impairs CAR-T cells in vitro. *Cancers (Basel)*, *11*, 602.

Betts, J. P. J., Warr, S. R. C., Finka, G. B., Uden, M., Town, M., Janda, J. M., … Lye, G. J. (2014). Impact of aeration strategies on fed-batch cell culture kinetics in a single-use 24-well miniature bioreactor. *Biochemical Engineering Journal*, *82*, 105–116.

Biasco, L., Scala, S., Basso Ricci, L., Dionisio, F., Baricordi, C., Calabria, A., … Aiuti, A. (2015). In vivo tracking of T cells in humans unveils decade-long survival and activity of genetically modified T memory stem cells. *Science Translational Medicine*, *7*, 273ra13.

Bohnenkamp, H., Hilbert, U., & Noll, T. (2002). Bioprocess development for the cultivation of human T-lymphocytes in a clinical scale. *Cytotechnology*, *38*, 135–145.

Calcinotto, A., Filipazzi, P., Grioni, M., Iero, M., De Milito, A., Ricupito, A., … Rivoltini, L. (2012). Modulation of microenvironment acidity reverses anergy in human and murine tumor-infiltrating T lymphocytes. *Cancer Research*, *72*, 2746–2756.

Caldwell, C. C., Kojima, H., Lukashev, D., Armstrong, J., Farber, M., Apasov, S. G., & Sitkovsky, M. V. (2001). Differential effects of physiologically relevant hypoxic conditions on T lymphocyte development and effector functions. *Journal of Immunology*, *167*, 6140–6149.

Carreau, A., Hafny-Rahbi, B. El, Matejuk, A., Grillon, C., & Kieda, C. (2011). Why is the partial oxygen pressure of human tissues a crucial parameter? Small molecules and hypoxia. *Journal of Cellular and Molecular Medicine*, *15*, 1239–1253.

Carswell, K. S., & Papoutsakis, E. T. (2000). Extracellular pH affects the proliferation of cultured human T cells and their expression of the interleukin-2 receptor. *Journal of Immunotherapy*, *23*, 669–674.

Corbet, C., & Feron, O. (2017). Tumour acidosis: From the passenger to the driver's seat. *Nature Reviews Cancer*, *17*, 577–593.

Costariol, E., Rotondi, M., Amini, A., Hewitt, C. J., Nienow, A. W., Heathman, T. R. J., … Rafiq, Q. A. (2019). Establishing the scalable manufacture of primary human T-cells in an automated stirred-tank bioreactor. *Biotechnology and Bioengineering*, *116*, 2488–2502.

Darja, O., Stanislav, M., Saša, S., Andrej, F., Lea, B., & Branka, J. (2016). Responses of CHO cell lines to increased pCO2 at normal (37°C) and reduced (33°C) culture temperatures. *Journal of Biotechnology*, *219*, 98–109.

Dobson, G. P., Yamamoto, E., & Hochachka, P. W. (1986). Phosphofructokinase control in muscle: Nature and reversal of pH-dependent ATP inhibition. *American Journal of Physiology-Regulatory, Integrative and Comparative Physiology*, *250*, R71–R76.

Erecińska, M., Deas, J., & Silver, I. A. (2002). The effect of pH on glycolysis and phosphofructokinase activity in cultured cells and synaptosomes. *Journal of Neurochemistry*, *65*, 2765–2772.

Erra Díaz, F., Dantas, E., & Geffner, J. (2018). *Unravelling the interplay between extracellular acidosis and immune cells*. Mediators Inflamm. London, UK: Hindawi Publishing Corporation.

Finlay, D. K., Rosenzweig, E., Sinclair, L. V., Carmen, F. C., Hukelmann, J. L., Rolf, J., … Cantrell, D. A. (2012). PDK1 regulation of mTOR and hypoxia-inducible factor 1 integrate metabolism and migration of CD8+ T cells. *Journal of Experimetnal Medicine*, *209*, 2441–2453.

Gattinoni, L., Lugli, E., Ji, Y., Pos, Z., Paulos, C. M., Quigley, M. F., … Restifo, N. P. (2011). A human memory T cell subset with stem cell–like properties. *Nature Medicine (New York, NY, United States)*, *17*, 1290–1297.

Gerweck, L. E., & Seetharaman, K. (1996). Cellular pH gradient in tumor versus normal tissue: Potential exploitation for the treatment of cancer. *Cancer Research*, *56*, 1194–1198.

Gouble, A., Philip, B., Poirot, L., Schiffer-Mannioui, C., Galetto, R., Derniame, S., … Smith, J. (2014). In vivo proof of concept of activity and safety of UCART19, an allogeneic "Off-the-Shelf" adoptive T-cell immunotherapy against CD19+ B-cell leukemias. *Blood*, *124*, 4689.

Guy, H. M., McCloskey, L., Lye, G. J., Mitrophanous, K. A., & Mukhopadhyay, T. K. (2013). Characterization of lentiviral vector production using microwell suspension cultures of HEK293T-derived producer cells. *Human Gene Therapy Methods*, *24*, 125–139.

Hale, L. P., Braun, R. D., Gwinn, W. M., Greer, P. K., & Dewhirst, M. W. (2002). Hypoxia in the thymus: Role of oxygen tension in thymocyte survival. *American Journal of Physiology-Heart and Circulatory Physiology*, *282*, H1467–H1477.

Halperin, M. L., Connors, H. P., Relman, A. S., & Karnovsky, M. L. (1969). Factors that control the effect of pH on glycolysis in leukocytes. *Journal of Biological Chemistry*, *244*, 384–390.

Hemmerich, J., Noack, S., Wiechert, W., & Oldiges, M. (2018). Microbioreactor systems for accelerated bioprocess development. *Biotechnology Journal*, *13*, 1700141.

Iyer, R. K., Bowles, P. A., Kim, H., & Dulgar-Tulloch, A. (2018). Industrializing autologous adoptive immunotherapies: Manufacturing advances and challenges. *Frontiers in Medicine*, *5*, 150.

Kalos, M., Levine, B. L., Porter, D. L., Katz, S., Grupp, S. A., Bagg, A., & June, C. H. (2011). T cells with chimeric antigen receptors have potent antitumor effects and can establish memory in patients with advanced leukemia. *Science Translational Medicine*, *3*, 95ra73.

Kelly, W., Veigne, S., Li, X., Subramanian, S. S., Huang, Z., & Schaefer, E. (2018). Optimizing performance of semi-continuous cell culture in an ambr15^{TM} microbioreactor using dynamic flux balance modeling. *Biotechnology Progress*, *34*, 420–431.

Kershaw, M. H., Westwood, J. A., & Darcy, P. K. (2013). Gene-engineered T cells for cancer therapy. *Nature Reviews Cancer*, *13*, 525–541.

Kim, J. W., Tchernyshyov, I., Semenza, G. L., & Dang, C. V. (2006). HIF-1-mediated expression of pyruvate dehydrogenase kinase: A metabolic switch required for cellular adaptation to hypoxia. *Cell Metabolism*, *3*, 177–185.

Kimura, R., & Miller, W. M. (1996). Effects of elevated pCO_2 and/or osmolality on the growth and recombinant tPA production of CHO cells. *Biotechnology and Bioengineering*, *52*, 152–160.

Klarer, A., Marsh, M., Ranade, S., & Smith, D. (2017). Advancing the robust manufacture of T-cell therapies through the application of stirred tank bioreactors. https://www.distekinc.com/wp-content/uploads/2017/06/Advancing-the-Robust-Manufacture-of-T-Cell-Therapies-through-the-Application-of-Stirred-Tank-Bioreactors-Poster.pdf

Klarer, A., Smith, D., Cassidy, R., Heathman, T. R. J., & Rafiq, Q. A. (2018). Demonstrating scalable T-cell expansion in stirred-tank bioreactors. *Bioprocess International*, *16*, 6–14.

Kochenderfer, J. N., Somerville, R. P. T., Lu, T., Shi, V., Bot, A., Rossi, J., … Rosenberg, S. A. (2017). Lymphoma remissions caused by anti-CD19 chimeric antigen receptor T cells are associated with high serum interleukin-15 levels. *Journal of Clinical Oncology*, *35*, 1803–1813.

Kreye, S., Stahn, R., Nawrath, K., Goralczyk, V., Zoro, B., & Goletz, S. (2019). A novel scale-down mimic of perfusion cell culture using sedimentation in an automated microbioreactor (SAM). *Biotechnology Progress*, *35*(5), e2832.

Larbi, A., Zelba, H., Goldeck, D., & Pawelec, G. (2010). Induction of HIF-1α and the glycolytic pathway alters apoptotic and differentiation profiles of activated human T cells. *Journal of Leukocyte Biology*, *87*, 265–273.

Louis, C. U., Savoldo, B., Dotti, G., Pule, M., Yvon, E., Myers, G. D., … Brenner, M. K. (2011). Antitumor activity and long-term fate of chimeric antigen receptor-positive T cells in patients with neuroblastoma. *Blood*, *118*, 6050–6056.

Maude, S. L., Frey, N., Shaw, P. A., Aplenc, R., Barrett, D. M., Bunin, N. J., … Grupp, S. A. (2014). Chimeric antigen receptor T cells for sustained remissions in leukemia. *New England Journal of Medicine*, *371*, 1507–1517.

McLaughlin, L. M., & Demple, B. (2005). Nitric oxide–induced apoptosis in lymphoblastoid and fibroblast cells dependent on the phosphorylation and activation of p53. *Cancer Research*, *65*, 6097–6104.

McNamee, E. N., Korns Johnson, D., Homann, D., & Clambey, E. T. (2013). Hypoxia and hypoxia-inducible factors as regulators of T cell development, differentiation, and function. *Immunologic Research*, *55*, 58–70.

Medvec, A. R., Ecker, C., Kong, H., Winters, E. A., Glover, J., Varela-Rohena, A., & Riley, J. L. (2018). Improved expansion and in vivo function of patient T cells by a serum-free medium. *Molecular Therapy: Methods & Clinical Development*, *8*, 65–74.

Mordon, S., Maunoury, V., Devoisselle, J. M., Abbas, Y., & Coustaud, D. (1992). Characterization of tumorous and normal tissue using a pH-sensitive fluorescence indicator (5,6-carboxyfluorescein) in vivo. *Journal of Photochemistry and Photobiology*, *13*, 307–314.

Pampusch, M. S., Haran, K. P., Hart, G. T., Rakasz, E. G., Rendahl, A. K., Berger, E. A., … Skinner, P. J. (2020). Rapid transduction and expansion of transduced T cells with maintenance of central memory populations. *Molecular Therapy: Methods & Clinical Development*, *16*, 1–10.

Pilon-Thomas, S., Kodumudi, K. N., El-Kenawi, A. E., Russell, S., Weber, A. M., Luddy, K., … Gillies, R. J. (2016). Neutralization of tumor acidity improves antitumor responses to immunotherapy. *Cancer Research*, *76*, 1381–1390.

Porter, D. L., Hwang, W. T., Frey, N. V., Lacey, S. F., Shaw, P. A., Loren, A. W., … June, C. H. (2015). Chimeric antigen receptor T cells persist and induce sustained remissions in relapsed refractory chronic lymphocytic leukemia. *Science Translational Medicine*, *7*, 303.

Rameez, S., Mostafa, S. S., Miller, C., & Shukla, A. A. (2014). High-throughput miniaturized bioreactors for cell culture process development: Reproducibility, scalability, and control. *Biotechnology Progress*, *30*, 718–727.

Roddie, C., O'Reilly, M., Dias Alves Pinto, J., Vispute, K., & Lowdell, M. (2019). Manufacturing chimeric antigen receptor T cells: Issues and challenges. *Cytotherapy*, *21*, 327–340.

Sallusto, F., Lenig, D., Förster, R., Lipp, M., & Lanzavecchia, A. (1999). Two subsets of memory T lymphocytes with distinct homing potentials and effector functions. *Nature*, *401*, 708–712.

Sandner, V., Pybus, L. P., McCreath, G., & Glassey, J. (2019). Scale-down model development in ambr systems: An industrial perspective. *Biotechnology Journal*, *14*, 1700766.

Sewell, D. J., Turner, R., Field, R., Holmes, W., Pradhan, R., Spencer, C., … Dikicioglu, D. (2019). Enhancing the functionality of a microscale bioreactor system as an industrial process development tool for mammalian perfusion culture. *Biotechnology and Bioengineering*, *116*, 1315–1325.

Trivedi, B., & Danforth, W. H. (1966). Effect of pH on the kinetics of frog muscle phosphofructokinase. *Journal of Biological Chemistry*, *241*, 4110–4112.

Wang, X., Popplewell, L. L., Wagner, J. R., Naranjo, A., Blanchard, M. S., Mott, M. R., … Forman, S. J. (2016). Phase 1 studies of central memory-derived CD19 CAR T-cell therapy following autologous HSCT in patients with B-cell NHL. *Blood*, *127*, 2980–2990.

Wenger, R., Kurtcuoglu, V., Scholz, C., Marti, H., & Hoogewijs, D. (2015). Frequently asked questions in hypoxia research. *Hypoxia*, *3*, 35–43.

Wiegmann, V., Martinez, C. B., & Baganz, F. (2020). Using a parallel micro-Cultivation System (Micro-Matrix) as a process development tool for cell culture applications. *Methods in Molecular Biology*, *2095*, 69–81.

Wutz, J., Steiner, R., Assfalg, K., & Wucherpfennig, T. (2018). Establishment of a CFD-based k_La model in microtiter plates to support CHO cell culture scale-up during clone selection. *Biotechnology Progress*, *34*, 1120–1128.

Xu, S., Jiang, R., Mueller, R., Hoesli, N., Kretz, T., Bowers, J., & Chen, H. (2018). Probing lactate metabolism variations in large-scale bioreactors. *Biotechnology Progress*, *34*, 756–766.

Zhu, M. M., Goyal, A., Rank, D. L., Gupta, S. K., Boom, T. V., & Lee, S. S. (2008). Effects of elevated pCO_2 and osmolality on growth of CHO cells and production of antibody-fusion protein B1: A case study. *Biotechnology Progress*, *21*, 70–77.

SUPPORTING INFORMATION

Additional supporting information may be found online in the Supporting Information section.

How to cite this article: Amini A, Wiegmann V, Patel H, Veraitch F, Baganz F. Bioprocess considerations for T-cell therapy: Investigating the impact of agitation, dissolved oxygen, and pH on T-cell expansion and differentiation. *Biotechnology and Bioengineering*. 2020;117:3018–3028. https://doi.org/10.1002/bit.27468